Photon Antibunching and Collective Effects in the Fluorescence of Single Bichromophoric Molecules

Christian G. Hübner,[1,*] Gert Zumofen,[2] Alois Renn,[2] Andreas Herrmann,[3] Klaus Müllen,[3] and Thomas Basché[1]

[1]*Institut für Physikalische Chemie, Johannes Gutenberg-Universität, Welderweg 11, D-55099 Mainz, Germany*
[2]*Swiss Federal Institute of Technology, Physical Chemistry, CH-8093 Zurich, Switzerland*
[3]*Max-Planck Institut für Polymerforschung, Ackermannweg 10, D-55128 Mainz, Germany*

The fluorescence of individual pairs of perylenemonoimide chromophores coupled via a short rigid linker is investigated. Photon antibunching is reported, indicating collective effects in the fluorescence, which are further substantiated by the observation of collective triplet off times and triplet lifetime shortening. The experimental findings are analyzed in terms of singlet-singlet and singlet-triplet annihilation based on Förster type energy transfer. The results reported here demonstrate that the statistical properties of the emission light of isolated single quantum systems can serve as a hallmark of intermolecular interactions.

PACS numbers: 42.70.Jk

Single molecule spectroscopy (SMS) is increasingly considered for applications in physics, chemistry, and life sciences, but basic investigations of single quantum systems also attract the researchers' interest [1]. In particular, the temporal properties of photon emission from single molecules were the subject of numerous studies. Photon antibunching [2,3], stochastic fluorescence off times due to excursions of the molecule to the triplet manifold [4], and quantum jumps [5] have been reported. Recently, SMS has yielded novel insights into the electronic interactions in multichromophoric assemblies such as light-harvesting pigments [6], conjugated polymers [7], donor-acceptor substituted biopolymers [8], and dendrimers carrying a variable number of chromophores [9]. The optical and electronic properties of such systems are strongly influenced by dipole-dipole interactions between the chromophores, giving rise to excitonic splittings and/or incoherent Förster type energy transfer. The simplest type of molecular aggregates that allow a rigorous study of these important effects are dimers where two chromophores are connected by an either rigid or flexible spacer. A prominent example of the latter variety are donor-acceptor labeled macromolecules where fluorescence resonant energy transfer has been successfully applied to measure distances and distance fluctuations on the nanometer scale [10]. In this Letter, we report on single molecule studies of isolated dimers with two identical chromophores attached to a rigid linker group. We show that energy transfer processes between the chromophores give rise to collective effects, which are reflected in the unique statistical properties of the emission light of single quantum systems. The observed photon antibunching shows features characteristic for singlet-singlet annihilation while collective off times indicate singlet-triplet annihilation.

The experiments were carried out for benzilic bi-perylenemonoimide (BBPM) bichromophores, where two perylenemonoimide (PM) chromophores are linked by the benzil motif. Two similar skewed conformers were reported for BBPM with the long axes of the chromophores at a relative angle of 112.5° and 68.8°, respectively [11]. For both conformations the interchromophore distances in the range of 1.5–2.0 nm are well below the Förster radius $R_0 \approx 4.5$ nm for the resonant energy transfer between the PM molecules and large enough to prevent coherent coupling at room temperatures. Thus, a fast excitation hopping among the chromophores is expected. Thin film samples of ≈ 30 nm thickness were prepared by spin casting a toluene solution of BBPM (10^{-9} M) and poly(methyl methacrylate) (10 g/l) onto a glass microscope cover slide [12]. Single BBPM fluorescence intensities were recorded with a homebuilt confocal optical microscope [12]. An argon-krypton mixed gas laser operated at 488 nm wavelength was used for a circularly polarized continuous wave excitation of the fluorophores with an intensity of 20 kW/cm². Fluorescence photons were, after appropriate filtering, detected in a Hanbury-Brown and Twiss detection scheme [13]. Transient intensities were obtained by collecting the photon signals in bins of custom width. Fast start-stop electronics was applied to measure interphoton times. During the measurements the sample was held in vacuum at 10^{-6} Torr to minimize oxygen mediated photodestruction.

A time course of the fluorescence intensity of an individual BBPM molecule is exemplarily shown in Fig. 1. Four intensity levels are visible in the trace at the top of the figure. The lowest level at the beginning and the end of the trace corresponds to blocked laser light. After opening the shutter, the photon detection rate is approximately 400 kHz. A sudden intensity drop to 200 kHz is observed at 82 s. In a second step at 91 s the rate drops to 40 kHz, which is close to the background level of 25 kHz found in areas without fluorescence. We attribute the two sudden drops to photobleaching of the individual chromophores of the BBPM molecule [11]. In what follows we denote the first photobleaching step by B1 for convenience. A
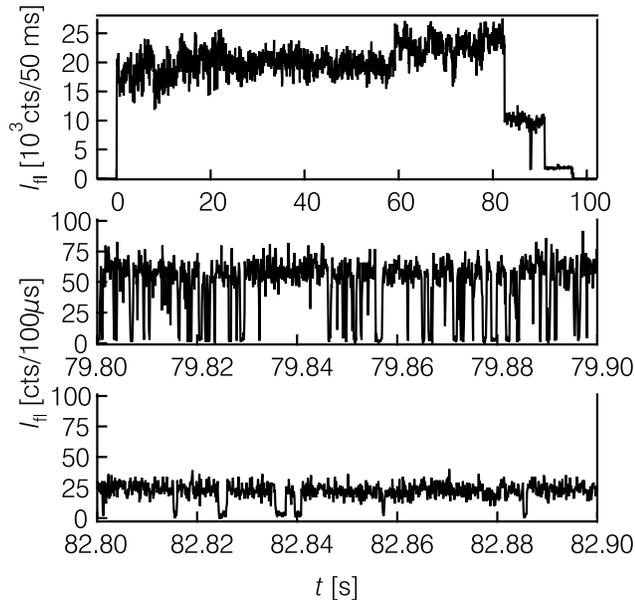
FIG. 1.   Transient fluorescence intensity of an isolated BBPM molecule. The top panel shows the whole time course of the fluorescence with a bin time of 50 ms demonstrating two-step photobleaching. In the two lower panels blowups before and after the first intensity drop at 82 s are displayed for a bin time of 100 μs.

FIG. 2.   Second order correlation functions $g^2(t)$ of the same molecule as in Fig. 1 before (squares) and after (circles) the first intensity drop at 81 s indicative of photon bunching in the microsecond range. The solid lines are fits to the function $1 + Ce^{-\lambda t}$.

reorientation of the chromophores can be ruled out as the origin of B1 because single PM chromophores attached to small dendritic residues showed only one-step behavior in independent experiments. Intensity fluctuations, as observed, for instance, at 60 s, are typical for these molecules and result presumably from slight configurational changes of BBPM [11]. Because of the distinct orientation of the two chromophores relative to the direction of light, the fluorescence intensity does not drop to half of the original intensity upon B1, in general. However, to simplify the analysis we focused on the symmetrical case by selecting molecules that showed an intensity reduction by a factor of approximately 2 upon B1 to assure that the two chromophores were excited at similar rates.

We now concentrate on the fluorescence time traces on enlarged scales in Fig. 1. The random-telegraph functions result from excursions of the BBPM to the triplet manifold [12]. Comparing the two time traces qualitatively, we note that on and off times are both longer after event B1 compared to before B1. A quantitative analysis can be performed by computation of the second-order correlation function $g^{(2)}(t)$ or by compiling off-time histograms. The result of the former method is visualized in Fig. 2. The fits to the function $1 + Ce^{-\lambda t}$ reveal contrasts C of 0.13 and 0.08 and lifetimes λ^{-1} of 0.25 and 0.60 ms before and after B1, respectively. In an approximate analysis these data can be related to the corresponding average on and off times $\tau_{\rm on}$ and $\tau_{\rm off}$ by $\lambda = \tau_{\rm on}^{-1} + \tau_{\rm off}^{-1}$ and $C = \tau_{\rm off}/\tau_{\rm on}$, yielding average on times of 2.0 and 7.3 ms and average off times of 0.29 and 0.60 ms before and after B1,

respectively. We also note that during the off times the fluorescence intensity reaches the background level before and after B1. The complete vanishing of the fluorescence during the off times when both chromophores are still intact indicates a collective behavior of the two chromophores, and accordingly the term collective off times is in use for this effect [9]. The collective behavior is assigned to singlet-triplet annihilation (STA), where the singlet excitation of one chromophore is efficiently quenched when the other chromophore is in the triplet state.

The average off times varied weakly from molecule to molecule and the corresponding histograms over the values for all molecules (not shown here) are peaked at 0.2 and 0.5 ms before and after B1, respectively. The values around 0.5 ms are assigned to the triplet lifetimes of individual chromophores attached to the benzilic moiety. Similar off times were found in the fluorescence from individual PM chromophores attached to a small dendritic residue in independent experiments. An explanation for the shorter triplet lifetimes before B1 is proposed below.

The on times show a different behavior. They vary strongly from molecule to molecule and take values of 0.7–6.3 ms and 1.8–32.0 ms before and after B1, respectively, in the present experimental data. They change by factors of 1–10 upon B1, and in almost all cases they increase by more than a factor of 2 as would be expected because of the reduced excitation probability by a factor of 2 when only one chromophore is active. Accounting for this factor the measurements tentatively indicate a further increase of the on times. We conclude that the intersystem-crossing (ISC) rate, limiting the on times, varies strongly between both chromophores, in agreement with a broad distribution of ISC rates found for individual PM chromophores. Thus, upon B1 the ISC rate and accordingly the on time may strongly change. Adopting the common idea that photobleaching occurs primarily during triplet excursions, it follows that the chromophore

with the larger ISC rate is more likely to be in the triplet state and to undergo photobleaching. Thus, the chromophore with the smaller ISC rate is likely to endure after B1 associated with an increase of the on times.

To obtain more information about energy transfer (ET) processes, interphoton times of the fluorescence were studied for periods before and after B1. Figure 3 shows the histogram of interphoton times before B1 for the same molecule as in Fig. 1. At short times, the interphoton time distribution follows the second-order correlation function $g^{(2)}(t)$. Note the different time scales between the bunching and antibunching regimes in Figs. 2 and 3. A pronounced dip at zero time difference is observed, indicating photon antibunching. The experimental data fit well a single exponential behavior from which a dip minimum of 0.13 and a fluorescence decay time of 4.35 ns is obtained. The experimental dip minimum A is clearly below 0.5, the value which would be expected for two independent and identical chromophores as discussed below. We conclude that efficient singlet-singlet annihilation (SSA) takes place so that simultaneous excitation of both chromophores is rapidly turned into a single excitation, and thus the probability for a coincident emission of two photons vanishes [14]. Histograms of dip minima $A = g^{(2)}(t = 0)$ are shown in Fig. 4 for BBPM and single PM chromophores. The histograms are peaked at 0.15 and range from 0.05 to 0.35. Dip minima A different from zero are thought to result from coincident background photons and from the finite time resolution of the avalanche photodiode detectors. Interphoton times were also recorded for the periods after B1 and compared with the interphoton times before B1. Within the experimental errors, $g^{(2)}(t)$ was the same before and after B1 in agreement with the predictions presented below.

For the discussion of the experimental observations we introduce simple model considerations. As mentioned above, at interchromophore distances of 1.5–2.0 nm fast incoherent ET processes take place at room temperatures and, thus, the excitation jumps resonantly between the two chromophores. The excitation hopping leads to
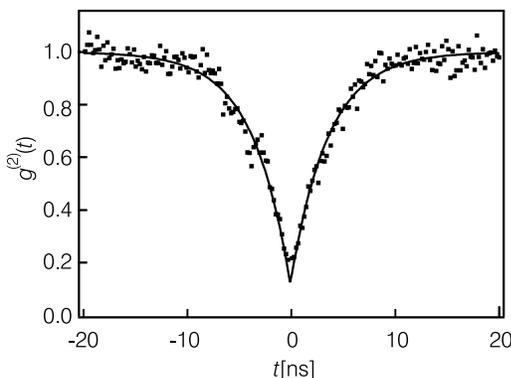
equal excited state populations of the two chromophores. Except for polarization effects, the resonant energy transfer is not supposed to cause significant collective effects in the fluorescence. Collective phenomena are expected when two electronic excitations in the dimer are simultaneously present. For singlet states we describe these processes in terms of a reaction scheme

$$
S_1^A + S_1^B \begin{cases} \nearrow & S_n^A + S_0^B \rightarrow S_1^A + S_0^B \\ \\ \searrow & S_0^A + S_n^B \rightarrow S_0^A + S_1^B, \end{cases} \tag{1}
$$
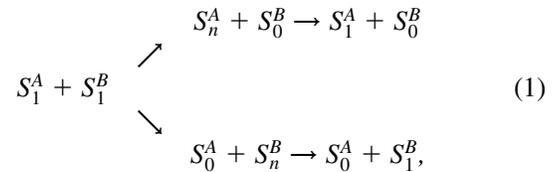
where, according to standard conventions, $S_0, S_1, \ldots$ denote the electronic ground and electronically excited singlet states, and the superscripts A and B denote the two chromophores. The first step is an energy up-conversion process mediated by Förster type ET while the second step denotes a fast intramolecular radiationless relaxation to the lowest singlet state S_1. The two steps represent SSA, which prevents the system from residing in a doubly excited state with both chromophores in the S_1 state. Consequently, after emission of a photon the system is in the ground state. Therefore, the second-order correlation function is zero at time zero, $g^{(2)}(0) = 0$. This is in agreement with the experimental data in Figs. 3 and 4 within the experimental limitations.

The photon statistics of the bichromophoric system can be analyzed in terms of rate equations and the second-order correlation function $g^{(2)}(t)$ can be given analytically. The expressions are rather lengthy and for clarity we present solely the main results for the symmetric case of two identical chromophores. However, we emphasize that the model applies also to the asymmetric case. In the two limiting cases where the SSA is faster than all other processes or where SSA is absent, $g^{(2)}(t)$ assumes the two limiting forms

$$
g^{(2)}(t) = \begin{cases} 1 - e^{-(2k_{01} + k_{10})t}, & \text{fast SSA} \\ 1 - \frac{1}{2} e^{-(k_{01} + k_{10})t}, & \text{no SSA.} \end{cases} \tag{2}
$$

FIG. 3. Second-order correlation function $g^{(2)}(t)$ recorded for the molecule of Fig. 1 before the first intensity drop showing photon antibunching in the nanosecond range.
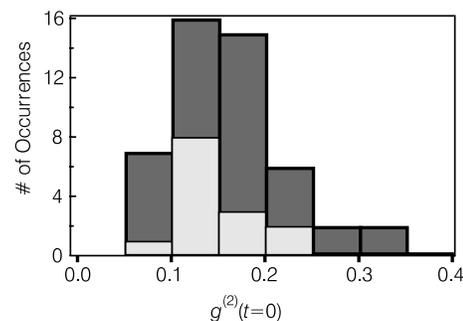
FIG. 4. Histogram of the $g^{(2)}(0)$ values obtained from the time traces of 50 bichromophores before the first intensity drop (dark bars). For comparison, the histogram of 14 single PM chromophores is also shown (light bars).

Here k_{01} is the single chromophore excitation rate and k_{10} is the sum of the radiative and radiationless relaxation rates. Both the prefactor and the relaxation rate are different in the two cases. However, usually the laser intensity is low (excitation rate $4 \times 10^6 \text{ s}^{-1}$), as in the present experiment, so that $k_{01} \ll k_{10}$ and the rates in Eq. (2) are dominated by k_{10}. To the contrary, the value of the dip minimum $g^{(2)}(0)$ is zero and $1/2$ in the two limiting cases and varies continuously between these two values for intermediate values of the SSA rate, independently of the laser power. The case of fast SSA, considered for the fit in Fig. 3, gives good agreement with the experimental data, taking into account the background fluorescence. Comparing the expression of fast SSA in Eq. (2) with the situation when only *one* chromophore is present, $g^{(2)} = 1 - e^{-(k_{01}+k_{10})t}$, both expressions differ solely in the rate. Again, for weak laser excitation, the rate is dominated by k_{10} and thus the expressions are identical. From these results no change of $g^{(2)}(t)$ in the antibunching regime is expected upon B1 in agreement with the observations.

Further ET and relaxation processes take place when singlet and triplet excitations are simultaneously present. As in Eq. (1) we describe these processes by a reaction scheme

$$S_1^A + T_1^B \rightarrow S_0^A + T_n^B \begin{array}{l} \nearrow \ S_0^A + T_1^B \\ \\ \searrow \ S_0^A + S_1^B, \end{array} \qquad (3)$$
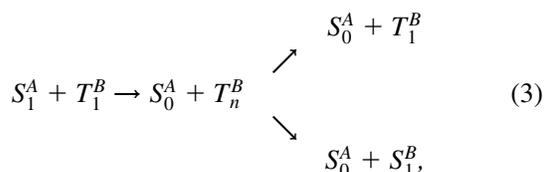
where T_1 denotes the lowest and T_n a higher electronically excited triplet state. As for the SSA the first step represents an energy up-conversion by Förster type ET followed by a fast radiationless relaxation step either to the lowest triplet state T_1 or, presumably, to the singlet state S_1. Both relaxation pathways are relevant. The first corresponds to singlet quenching (STA). If this process is faster than the fluorescence, the fluorescence vanishes completely when one chromophore is in the triplet state. This gives rise to the collective off times, as observed in Fig. 1. The other pathway leads to an accelerated reverse intersystem crossing and thus to a shortening of the off times. We propose this effect being responsible for the observed off-time shortening by a factor of $2-3$ when both chromophores are active.

We have considered three types of ET, namely, ET from one chromophore in the first excited singlet state to the other chromophore (i) in the ground state (energy hopping), (ii) in the first excited singlet state (SSA), and (iii) in the first excited triplet state (STA), where the latter two are associated with energy up-conversion and population of higher singlet or triplet states. The efficiency of these processes depends on the spectral overlap of the emission and absorption spectra of the transitions into which the ET transfer process can be decomposed. It is

the overlap of the $S_1 \rightarrow S_0$ fluorescence and the $S_1 \leftarrow S_0$, the $S_n \leftarrow S_1$, and the $T_n \leftarrow T_1$ absorption spectra for energy hopping, SSA, and STA, respectively. All spectra except the $S_n \leftarrow S_1$ absorption spectrum are known for PM [15], yielding transfer rates of ≈ 30 GHz for energy hopping and ≈ 750 GHz for STA. The latter is much faster than the fluorescence rate of ≈ 0.2 GHz, a precondition for complete STA as observed in Fig. 3. For SSA, a transfer rate of 100 GHz was recently reported [16] supporting our interpretation of the antibunching data.

Förster type energy transfer, which depends to the sixth power on the interchromophore separation, constitutes a molecular ruler to measure distances in the nanometer range. Our investigations suggest that by a controlled increase of the interchromophore distance the contrast of the antibunching signal gradually approaches the value of 0.5 of uncoupled chromophores. Similar to the experiment in Ref. [10], our results indicate that the antibunching signal can be applied to investigate conformational fluctuations of, say, chromophore-pair labeled macromolecules, where the disadvantage of a possibly smaller Förster radius as compared to a specifically chosen donor-acceptor pair is outweighed by the chemistry, which is usually much easier to accomplish for the homolabeling.

*Electronic address: chuebner@mail.uni-mainz.de
[1] *Single Molecule Spectroscopy*, edited by R. Rigler, M. Orrit, and T. Basché, Chemical Physics Vol. 67 (Springer, Berlin, 2002).
[2] T. Basché, W. E. Moerner, M. Orrit, and H. Talon, Phys. Rev. Lett. **69**, 1516 (1992).
[3] L. Fleury *et al.*, Phys. Rev. Lett. **84**, 1148 (2000).
[4] J. Bernard, L. Fleury, H. Talon, and M. Orrit, J. Chem. Phys. **98**, 850 (1993).
[5] T. Basché, S. Kummer, and C. Bräuchle, Nature (London) **373**, 132 (1995).
[6] A. M. van Oijen *et al.*, Chem. Phys. **247**, 53 (1999).
[7] D. A. VandenBout *et al.*, Science **277**, 1074 (1997).
[8] T. Ha *et al.*, Proc. Natl. Acad. Sci. U.S.A. **93**, 6264 (1996).
[9] J. Hofkens *et al.*, J. Am. Chem. Soc. **122**, 9278 (2000).
[10] A. J. Berglund, A. C. Doherty, and H. Mabuchi, Phys. Rev. Lett. **89**, 068101 (2002).
[11] T. Christ *et al.*, J. Lumin. **98**, 23 (2002).
[12] C. G. Hübner, A. Renn, I. Renge, and U. P. Wild, J. Chem. Phys. **115**, 9619 (2001).
[13] R. Hanbury-Brown and R. Twiss, Nature (London) **177**, 27 (1956).
[14] M. Wu, P. M. Goodwin, W. P. Ambrose, and R. A. Keller, J. Phys. Chem. **100**, 17 406 (1996).
[15] T. Vosch *et al.*, Angew. Chem., Int. Ed. Engl. **40**, 4643 (2001).
[16] G. De Belder *et al.*, Chem. Phys. Chem. **2**, 49 (2001).